

# **NASA CONTRACTOR REPORT 181686**

## **FRACTURE CHARACTERISTICS OF BALLOON FILMS**

**M. A. Portanova**  
**Contract NAS1-18000**  
**PRC Kentron, Inc.**  
**Hampton, VA**

**(NASA-CR-181686) FRACTURE CHARACTERISTICS**  
**OF BALLOON FILMS (PRC Kentron) 36 p**  
**CSCL 11C**

**N89-21099**

**Unclas**  
**G3/27 0191711**

**JANUARY 1989**



**National Aeronautics and  
Space Administration**

**Langley Research Center**  
**Hampton, Virginia 23665-5225**

## TABLE OF CONTENTS

	<u>Page</u>
INTRODUCTION .....	1
KEY WORDS .....	2
NOMENCLATURE .....	3
TEST EQUIPMENT AND PROCEDURES .....	4
SPECIMENS .....	7
RESULTS AND DISCUSSION .....	9
UNIAXIAL TESTING .....	9
FRACTURE TOUGHNESS TESTS .....	11
CONCLUSION .....	18
REFERENCES .....	20
FIGURES .....	21

## Introduction

Heavy lift, high altitude polyethylene scientific balloons have shown themselves to be both a reliable and economical means for conducting atmospheric research. Scientific ballooning, which celebrated its 50'th anniversary recently, has never had a success ratio that approached 100 %. This is due, in part, to the nature of scientific experimentation where each advancement in balloon capability is met with either a greater demand in payload or float altitude. In recent years, however, 80 to 90 percent of the flights have been failures. These failures have primarily occurred during the ascent through the troposphere. Because of this extremely high failure rate a number of investigations have been initiated to determine the probable cause of failure.

For most missions, the balloons pass through the troposphere where the temperature can be as low as  $-60^{\circ}\text{C}$ . The polyethylene films are formulated to have a glass transition temperature or Cold Brittleness Point (C.B. point) below this minimum flight temperature. As a result, the films will have a plastic or ductile behavior through the flight regime. The reported temperature for the C.B. point was  $-83.^{\circ}\text{C}$  for the Stratafilm and  $-96^{\circ}\text{C}$  for the Astrofilm.

Most of the failures took place in the troposphere. Thus, a high C.B. point was suspected to be a principle cause of the failures. The primary focus of

this investigation was to determine the effects of decreasing temperature on the notch sensitivity of the films. To this end, slits of various lengths were cut in test samples and uniaxial loads were applied perpendicular to the slits. Test temperature ranged from 23° C (room temperature) to -120°C. Values of fracture toughness were calculated for each temperature. Stress-strain tests, of unnotched specimens were also conducted to support calculations of fracture toughness.

#### Key Words

High altitude balloons, Polyethylene film, Notch sensitivity, Crack propagation, Tropopause.

## NOMENCLATURE

a	Half length of crack, in
b	Specimen width, in.
a/b	Ratio of half crack length to sample width
A	Cross-sectional area, in <sup>2</sup>
E	Young's Modulus of elasticity, psi
E <sub>sec</sub>	Secant Modulus, ksi
g	Gravitational acceleration, $\frac{\text{in}}{\text{sec}^2}$
G	Strain energy release rate, $\frac{\text{in lbs}}{\text{in}^2}$
G <sub>c</sub>	Critical value of strain energy release rate, $\frac{\text{in lbs}}{\text{in}^2}$
G <sub>sec</sub>	Pseudo value of strain energy release rate, $\frac{\text{in lbs}}{\text{in}^2}$
h	Height, in
K	Stress intensity factor, psi $\sqrt{\text{in}}$
K <sub>c</sub>	Critical value of stress intensity factor, psi $\sqrt{\text{in}}$
$\hat{K}_c$	Average critical value of the stress intensity factor, psi $\sqrt{\text{in}}$
L	Length, in
m	Mass, slug
P	Line load, lbs
v	Velocity, in/sec
$\sigma$	Normal stress, psi
$\epsilon$	Normal strain,
$\pi$	Transcendental irrational number

### Test Equipment and Procedure

For these polyethylene films the stress-strain curve is highly dependent upon strain rate. Because the balloon structure is subject to dead-weight loading all tests were conducted at a constant load rate as opposed to a constant displacement rate.

All Astrofilm and Stratafilm test specimens came from a single sample lot supplied by Wallops Flight Facility. The Astrofilm was designated "Astro-E", and the Stratafilm was designated "SF-85". Both films were 0.8 mils thick.

Samples were uniaxially loaded to failure in a special loading apparatus constructed exclusively for testing polyethylene film at controlled environmental conditions. The ends of the specimens were clamped between two rubber lined low mass thermoplastic polymer (polymethylmethacrylate) plates. This method firmly but gently grips the film sample and minimizes the number of wrinkles in the test sample. Also the grips cool down to test temperature in a relatively short period of time, expediting the testing. All loads were increased monotonically in the extruded direction.

Test conditions were maintained in a specially designed environmental chamber which consisted of a rectangular plywood box with an inner liner made of 1100 series aluminum. A half inch of Styrofoam insulation was placed between the plywood and aluminum, on the plywood side of the box. A 3/8 inch diameter copper tube inside the bottom of the air space, on top of the insulation, introduced liquid nitrogen ( $LN_2$ ) to cool the chamber. The copper tube

"diffuser", which twice traversed the bottom of the box, contained small holes that allowed  $\text{LN}_2$  to escape every inch of tube length. This method gave uniform temperature and allowed rapid cooling of the test chamber. The liquid nitrogen input was controlled by a solenoid activated by four internally mounted T type (copper constantan) thermocouples. Aluminum structural angle was attached to the bottom of the test chamber to stiffen the floor. Also, the extra mass helped to stabilize the temperature after cool down. A test temperature could be maintained as low as  $-150^\circ \text{C}$ . The internal dimensions of the test chamber were 11 in. wide X 7 in. deep X 48 in. long. In order to reduce moisture in the test chamber, nitrogen vapors were allowed to create a slight positive pressure inside the test chamber. This low moisture level helped maintain a low temperature differential over the test chamber.

For each test, the test chamber and grips were cooled to the testing temperature. The specimen was installed in the pre-cooled grips and placed in the test chamber. The time required to achieve the testing temperature generally took less than three minutes but five minutes was always allowed. One grip was pinned to allow rotation about its center, insuring proper specimen alignment. The other grip was attached to two parallel cables, which ran over a series of Teflon pulleys to a load cell outside the test chamber. Load was then applied at a constant rate of 3.2 lbs/min by filling a small container with water which was attached to the load cell. A Linear Variable Differential Transformer (LVDT), mounted outside the test chamber, was used to measure the displacement of the test specimen. An X-Y plotter was used to record load verses displacement. Although the system was closed to the environment during testing, a clear 3/8 inch thick plexiglass lid permitted observation of the specimen.

Unnotched stress-strain data could not be obtained with this testing apparatus because the displacement measurements did not give accurate strains over the large range of displacements. At room temperature, strains in the 1000 % range were not uncommon. A typical servohydraulic load control testing machine does not have a sufficient actuator stroke length. An Instron model 4200 screw driven machine, which has a large displacement capacity, was chosen. This testing machine was interfaced with an HP-45 personal computer. A closed loop control program was written to control the constant strain rate machine as if it were a constant load rate machine. The control program varied the crosshead displacement speed to maintain the required load rate. The program worked fairly well except at room temperature when the film flowed faster than the screwhead speed capacity. Consequently, the load rate in the plastic region of the stress-strain curves at room temperature was as low as 2.9 lbs/min compared to the initial 3.2 lbs/min. Also, at the colder temperatures the actual load periodically overshoot the required load rate and the crosshead displacement had to be slowed or almost stopped in order for the desired load to converge with the actual load. This resulted in a sawtooth appearance near the end of the stress-strain curves. It should be emphasized that this sawtooth appearance is purely an artifact of the load control program, not a characteristic of the material. This problem was not considered serious because the data from these regions was not used in the analysis.

To conduct the cold stress-strain tests in the Instron, an aluminum test chamber was constructed to enclose the specimen and grips. This inner chamber was then enclosed inside a larger aluminum outer chamber and liquid nitrogen (  $LN_2$  ) was introduced in the annulus to cool the specimens. Nitrogen introduction was controlled by internally mounted thermocouples, which were



solenoid activated. Test specimens were installed in the pre-cooled grips and then allowed to cool to test temperature. The load cell was zeroed before each test and a pretension of approximately 0.01 lbs was placed on the specimen to ensure that the specimen was taut. Test data was stored on magnetic floppy media and was transferred via a IEEE-RS232 interface to an IBM PC for reduction.

### Specimens

A study was conducted to determine the best test specimen configuration because testing methods for measuring strength have not been standardized by ASTM for balloon films. Wishbone-shaped specimens with various widths and fillet radii and straight sided rectangular test specimens with various widths were tried. It was found that the production of wishbone shaped specimens was a time consuming and tedious task and failures were often questionable. Only rectangular test coupons were used in this parametric study. Stresses were calculated using the nominal thickness of 0.8 mils. Actual thicknesses ranged from 0.72 to 0.84 mils.

Unnotched Test Specimens: The test specimens were 1 in. by approximately 12 in. with a nominal thickness of 0.8 mils. An average of 8 replicate tests were run at each testing temperature.

Notched Test Specimens: The test specimens were 3 in. by approximately 12 in. A template was used to cut the notches uniformly. The notch lengths (2a) were 0.1, 0.3, 0.7, 1.0 in. giving respective values of a/b of 0.033, 0.100, 0.233,

and 0.333. Stress concentrations generated by the grips or edge notches were not critical because the stress concentration at the crack tip assured failure from the notch. A range of 8 to 12 replicate tests were run for each notch length on both films at all testing temperatures.

**Stress Strain Test Specimens:** The specimens were 1 in. by 5 in. Usually 8 to 10 replicate tests were run at each testing temperature for both films.

## Results and Discussion

Uniaxial Tests: A comparison of ultimate strengths for various specimen widths was made at room temperature. The test specimen length was held constant at 12 in. due to equipment constraints. The specimen width was varied between 0.5 and 4.0 inches. This study revealed two predominant effects that influenced selection of the final test specimen configuration - grip effects and edge effects.

A plot of strength verses specimen width is shown in Figure 1. The strength is maximum for a specimen width of 1 in. Thus, a test specimen of 1 in. by 12 in. was chosen. The reduction in strength as width increases is probably the result of high local stresses generated by grip effects. This stress concentration is due to the Poisson effect and the inability of the material to contract inside the grips. This restriction in material flow introduces a biaxial tension-tension state of stress in the specimen in the vicinity of the grips. In fact, short-wide specimens are used for biaxial specimens. The reason for the narrowest specimen being weakest is not obvious.

Small nicks at the films edge acted like a notch to reduce strength. Thus, specimen preparation was very important. Nick-free edges were best made by placing the polyethylene film between two pieces of backing material and making each cut on a glass plate with a fresh razor blade.

Once the test specimen configuration was established tests were conducted to rank the two film types. Figure 2 is a plot of failing strength of both films verses increasing temperature. This graph shows that the strength of both films increase dramatically with decreasing temperature. The difference between films is small. Thus, the balloon should be capable of withstanding greater loads at altitudes where the cold temperatures are encountered. However, this trend is inconsistent with the preponderance of balloon failures in the troposphere.

Stress-Strain tests were run at various temperatures on both films. Because of the extremely high strain at failure, it was necessary to use the shortest specimens possible. A series of tests were run for various specimen lengths and for a constant width of 1.0 in. The stress-strain results are plotted in Figure 3. Each of these curves are an average of 6 to 10 tests. The ultimate strain shown is the minimum failing strain for each set of tests. As shown in Figure 3, the yield strength for the 4 and 5 in. gage length is slightly greater than that for the 3 and 6 in. gage lengths but the differences are not significant. Because the average failing strengths were within 5 percent of values obtained with 12 inch long specimens of the same width as in Figure 1, any specimen length between 3 and 12 inches is acceptable. A gage length of 5 inches was chosen so that the displacements at maximum strain would be near the extension limits of the testing machine.

Figure 4 is a composite display of stress verses strain data for both films at each of the testing temperatures. Again little difference is found between the two films. The scales for each of the plots are the same to show the significant change in strength and failing strain with changes in temperature.

At room temperature the strengths are low but failing strains are extremely high. This ductile behavior diminishes as temperature decreases until at the colder temperatures the stress-strain behavior resembles that of a brittle material. The ultimate strength increases from approximately 2,000 psi to greater than 11,000 psi at the coldest temperature. Figure 5 is a plot of the same data but the horizontal scale has been expanded to better display the fine differences in the stress-strain relationships at the colder temperatures. The Astrofilm can be seen to be slightly tougher than the Stratafilm for three of the four temperatures.

**Fracture Toughness Tests:** An investigation of the films sensitivity to cuts or notches was the primary objective of this research. For this series of tests 3 in. wide by 12 in. long specimens were used. Various widths were tried but it was found that a wider specimen gave both a good width to notch length ratio ( $a/b$ ) and was easy to produce. Narrow specimens tended to fail prematurely due to edge notch effects and the length to width ratio was difficult to maintain and still keep the same ratio of width to notch lengths. This study showed that biaxial grip effects were not present with the 3 in. specimen.

The majority of the flight failures have been in balloons constructed from Stratafilm. The plots of the notched strength verses notch length at several test temperatures, Figure 6, illustrate that there is not a great deal of difference in the notch sensitivity of the two films. In all tests, the Astro-E film is slightly stronger than the Stratafilm; however, the difference is not large enough to explain why the Stratafilm balloons have had a much

greater failure rate. The failing strengths increase with decreasing temperature, much as the unnotched specimens. Notice though that the strength decreases sharply with the introduction of the smallest cut. At room temperature the ultimate strength may fall below the design "stress index" levels used by today's balloon designers. Even so, the majority of balloon failures were not at low altitudes and warmer temperatures but at colder, tropopause conditions. (This "Stress Index" is calculated for a simple shell with internal pressure and accounts for payload and film thickness. It is not derived from a detailed stress analysis of the balloon nor is it a measured value. It only represents a working index used to judge relative performance.)

Notch sensitivity trends were established using linear elastic fracture mechanics (LEFM). The film was assumed to be an isotropic elastic material. The films were only slightly anisotropic but very viscoplastic. Even so, the trends for toughness should be valid.

Linear elastic analysis forms the basis of most fracture analyses when the plastic zone at the crack tip is small and constrained by the surrounding linear-elastic region. In most circumstances the fracture toughness of a material is characterized through the use of a crack tip stress intensity factor  $K_c$ . This stress intensity factor represents the strength or level of the singular stress field near the crack tip. It has been shown by Paris and Sih [1] that the stress intensity factor for a central crack in a sheet of finite width is

$$K_c = \sigma \sqrt{\pi a} * F(a/b) \quad (1)$$

Where

$$F(a/b) = \sqrt{(2b/a) * \tan(a/2b)}$$

with better than 5% accuracy for  $a/b \leq 0.5$

The thin balloon films cannot support compressive stresses that develop above and below the crack face between the crack tips. These compressive stresses cause wrinkles above and below the cracks. The SIF for such a problem has not been determined. Thus, the accuracy of eq. (1) cannot be assessed by analysis. However, examination of Figure 7, a log-log plot of the failing strength versus the notch length, shows that the slope of the regression lines approximates the inverse square root function in equation (1) for long notches. For short notches the data does not follow linear elastic fracture mechanics (LEFM). Most materials do not follow LEFM for short cracks. Thus, the values of  $K_c$  calculated with eq. (1) will be in error by a geometric factor which should be independent of film material and temperature.

The notch strength data in Figure 6 is replotted on a log-log plot in Figure 8 for each of the testing temperatures. The straight lines drawn in Figure 8 are linear regression lines fit to the notch strength data for the long cracks. The slopes of these lines are close to  $-\frac{1}{2}$  which suggest that equation 1 may be used to interpret the test data. It can be seen that at the colder temperatures the agreement of the regression line is better than at room temperature. This is due in part to the increase in stiffness of the material

and it's loss of ductility. Figures 9 and 10 are also log-log plots of the notched strength verses notch length for each of the materials at all four testing temperatures. These graphs allow a comparisons of the effects of temperature on each film.

The stress intensity factor at failure,  $K_{Ic}$ , gives the level or intensity of the elastic stress field around the crack tip in the case were the strains are purely elastic [Ref. 2]. In real materials a plastic zone generally forms at the crack tip. If crack size is large relative to plastic zone size, the stress intensity factor still describes the stresses near the crack tip but not at the crack tip. In testing any viscoelastic material attention should be paid to crack tip plasticity and other non-linear effects. When plasticity is more extensive relative to the size of the crack,  $K$  loses it's significance. This size effect was evident in Figure 8; when the crack is small, the fit of the regression line to the elastic theory is poor.

The average fracture toughness,  $K_{Ic}$ , is plotted against temperature in Figure 11. The film gets continuously tougher with decreasing temperature. This behavior is not typical for most engineering materials as shown in Ref.3. In metals the value of  $K_{Ic}$  usually decreases with decreasing temperature. For some aluminums,  $K_{Ic}$  increases slightly with decreasing temperature, but nothing like that in Figure 11.

The Modulus of Toughness, a measure of the unnotched toughness of the film, is plotted against temperature in Figure 12. The Modulus of Toughness is the work per unit volume required to cause fracture. It is calculated as the area under the stress strain curve up to the point of fracture. In contrast to the



fracture toughness in Fig 11, the Modulus of Toughness decreases with decreasing temperature much like that for metals. As temperature decreases, failing strains or ductility decreases but strength increases. See Figures 4 and 5. The ductility dominates, causing the Modulus of Toughness to decrease. As the Modulus of Toughness decreases, the failure may change from ductile to brittle.

In metals, the Charpy Impact method is often used to determine the transition from ductile to brittle behavior. In the ballooning industry, the Falling Ball Test is used to measure the transition from ductile to brittle behavior. A steel ball is dropped from a given height onto a circular piece of polyethylene film that is clamped around it's circumference. The ball drop height is increased until the ball penetrates the film, rather than being caught by it. The first test temperature is a little warmer than the suspected transition temperature or Cold Brittleness Point. The test is repeated at small increments of decreasing temperature. The fractured area is inspected after each test. If the fracture bifurcates the failure is deemed brittle, if not then it is deemed ductile. The Cold Brittleness Temperature is the temperature at the transition. For the films stated here the C.B. points are -83 °C for the Stratafilm and -96 °C for the Astrofilm. In Figure 12, the modulus of toughness reaches a minimum value around the C.B. temperature. Thus, the Modulus of Toughness and C.B. point appear to be consistent.

Another measure of notched toughness is the strain energy release rate  $G_c$ . The rate  $G_c$  is defined as the total elastic energy available during fracture per unit crack extension to propagate the crack [Ref. 4]. Under linear elastic conditions

$$G_c = \frac{K_c^2}{E} \quad (3)$$

However, the balloon film is not linear elastic. The non-linearity can be taken into account in an approximate fashion using the secant modulus.

Replacing  $E$  by  $E_{sec}$  in equation (3),

$$G_{sec} = \frac{K_c^2}{E_{sec}} \quad (4)$$

where  $E_{sec} = \frac{\sigma_{max}}{\epsilon_{max}} \quad (5)$

The change in the kinetic energy of the ball as it passes through the film is proportional to the strain energy release rate associated with fracture of the film. It is therefore postulated that the strain energy release rate, determined from the notch strength tests, using equation 4 is related to the falling ball test used in the ballooning industry.

Figure 13 is a plot of  $G_{sec}$  versus the inverse of temperature.  $G_{sec}$  was calculated with equation 4 and  $K_c$  was obtained from the data in Figure 11. The  $G_{sec}$  reaches a peak value rather than continuing to increase with decreasing temperature like  $K_c$  in figure 11. The values of  $G_{sec}$  in Figure 13 peak at about the same temperature as the reported Cold Brittleness Temperatures for these materials. Thus, the peak  $G_c$  appears to correspond to the transition from ductile to brittle behavior as indicated by the falling ball test.

Both  $K_c$  and  $G_c$  are measures of toughness. Usually one is consistent with the other. However, they are not consistent here with regard to changing

temperature. Below the Cold Brittleness Temperature the strength of the flawed films increase with decreasing temperature; whereas, the energy absorbed decreases with decreasing temperature. In either case, the toughness of the films increases with decreasing temperature up to the cold brittleness point, which is below the average temperature encountered in the tropopause. Thus, films with crack-like flaws are no more likely to fail in the tropopause than unflawed films.

### Conclusions

In general the results of the experiments show that the strengths of the balloon films are reduced significantly by crack-like flaws. The notched strengths at room temperature are below the design stress index level, implying that a cut or tear in the balloon membrane could cause premature failure. On the other hand, the fracture toughness (stress intensity factor at failure) increases with decreasing temperature down to  $-120^{\circ}\text{C}$ . Thus, as the balloon ascends and the temperature decreases the notched strength increases to values above the stress index levels. These results tend to rule out the possibility that failures in the tropopause are caused by crack-like tears in the film.

It was shown that the trend in the strain energy release rates determined from the notched strength tests correlated with the results from the ball drop test, which is a standard test used in the ballooning industry for measuring transitions from ductile to brittle behavior. In contrast to the fracture toughness, the strain energy release rate reached a peak value at the same temperature as the Cold Brittleness Point,  $-83^{\circ}$  to  $-96^{\circ}\text{C}$ .

The uniaxial tensile test and notched strength test results of this study do not point to a materials integrity problem for either of the two investigated balloon films. Furthermore, the test results suggest that the films are more likely to fail prematurely due to crack-like flaws on the ground, at warmer temperatures, than in the tropopause where most of the premature failures have

occurred. It is recommended that a similar investigation be conducted to determine the effects of a biaxial stress state on the strength and toughness of the films. Also, the strength of the film with repaired flaws resulting during manufacturing should be investigated.

## REFERENCES

- [1] "Stress analysis of cracks", Fracture Toughness Testing and it's Applications. ASTM Special Technical Publications No.381. edited by Paris and Sih, June 21-26, 1964, pp. 2.1-2.3.
  
- [2] Barrett, C.R.; Nix, W.D.; Tetelman, A.S.: The Principles of Engineering Materials. Prentice-Hall, Inc., 1973, pp. 282-290.
  
- [3] Broek, D.: Elementary Engineering Fracture Mechanics, Third ed. Martinus Nijhoff Publishers, 1982, Chapter 7, pp. 170-184.
  
- [4] Popov, E.P.: Mechanics of Materials, second ed. Prentice-Hall, 1976, pp. 525-528.
  
- [5] Beer, F.P.; Johnston, E.R.: Mechanics of Materials. McGraw-Hill Book Company, 1981. pp. 3-4

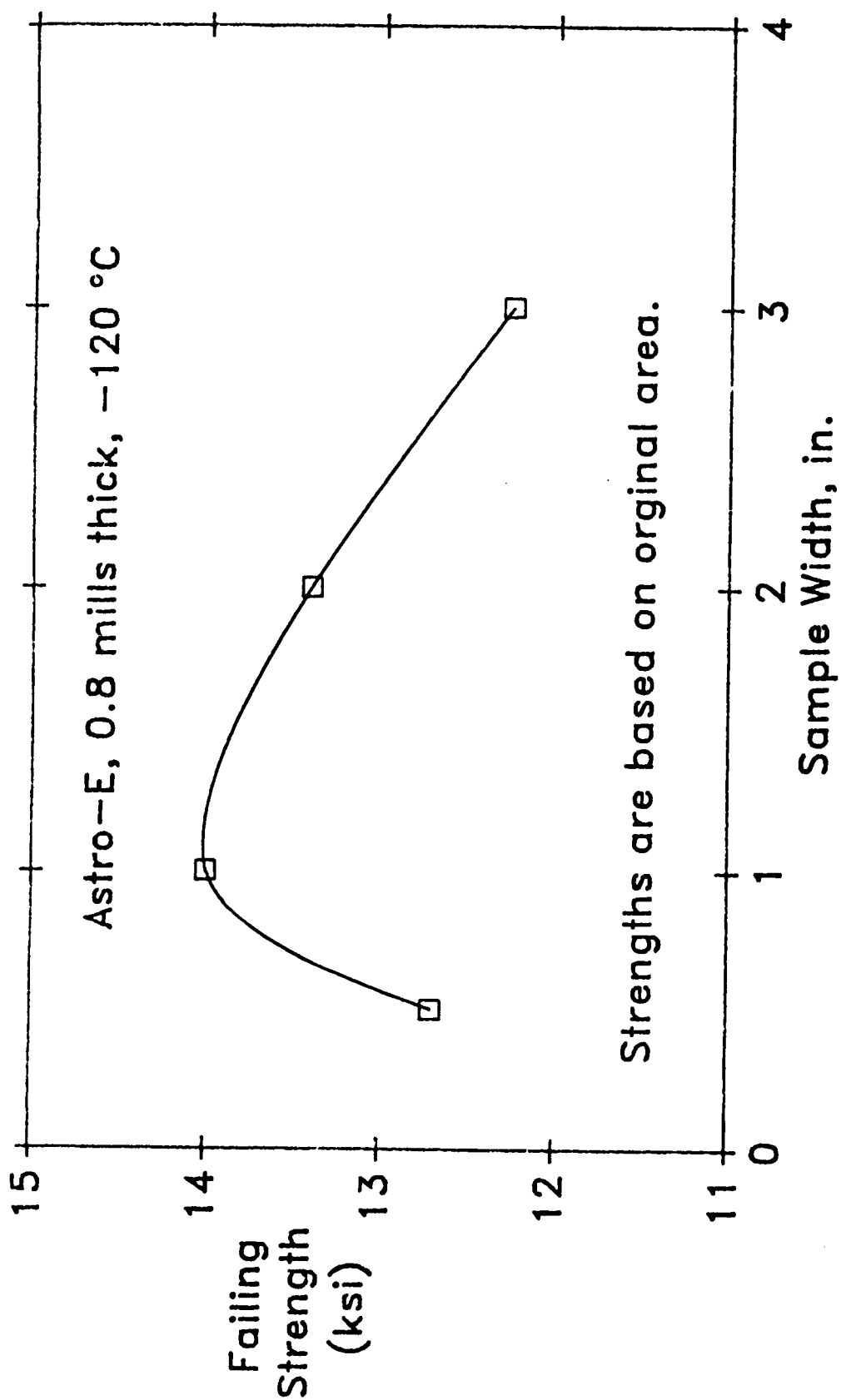


Fig 1: A comparison of failing strength to sample width

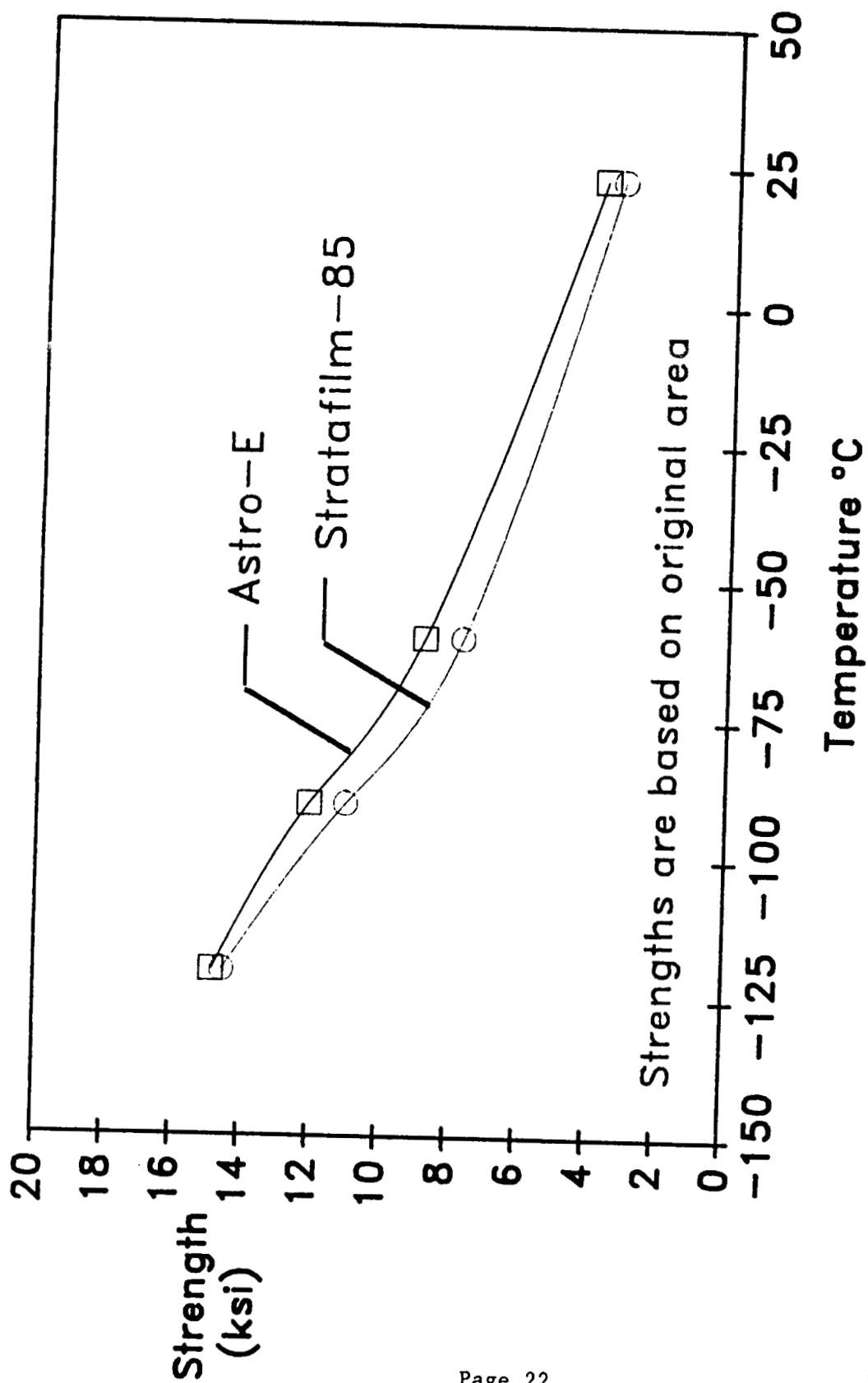


Fig 2: A comparison of failing strength versus temperature



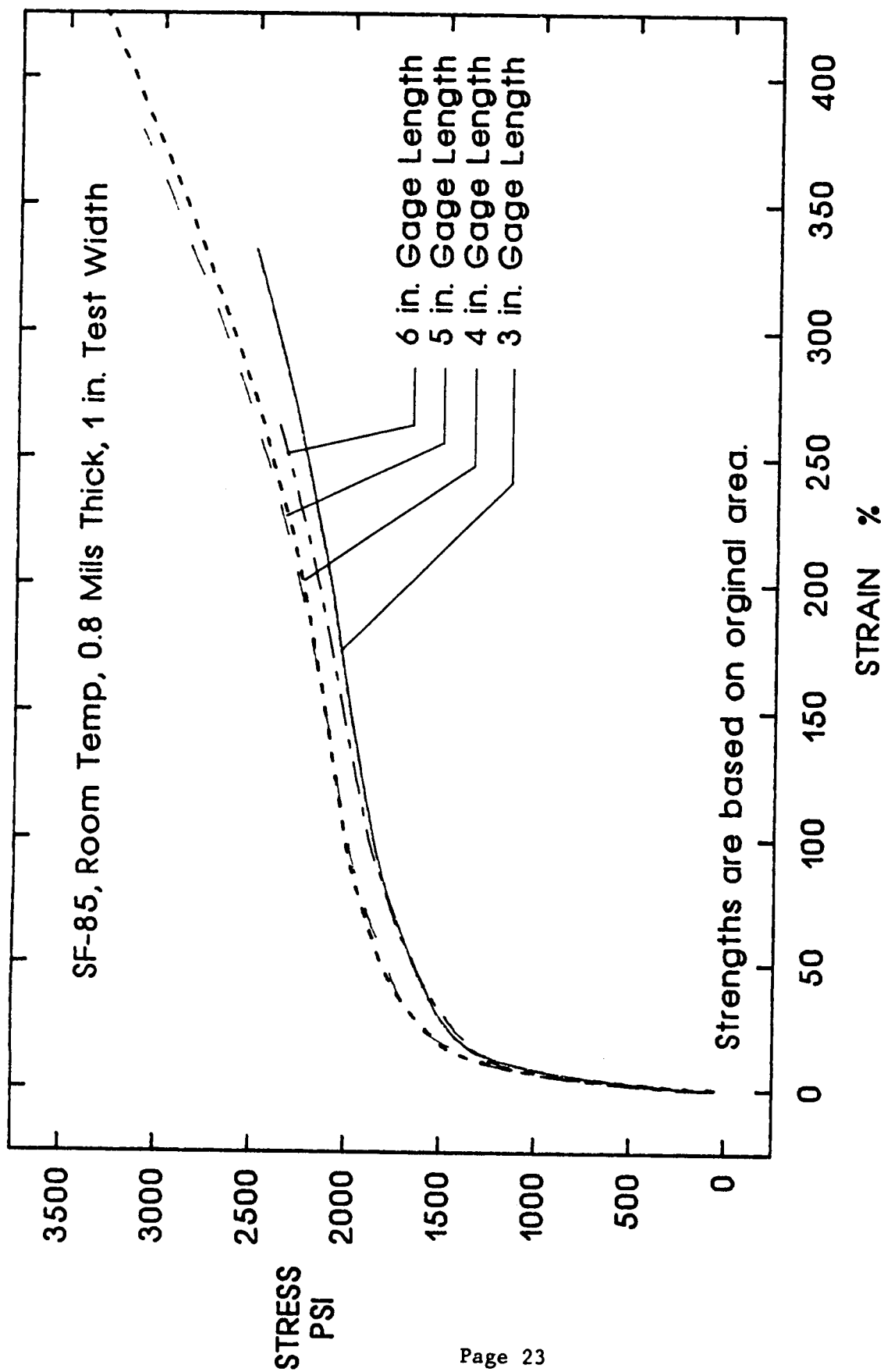


Fig 3: A Parametric Study of The Effects  
of Far-Field Stresses.

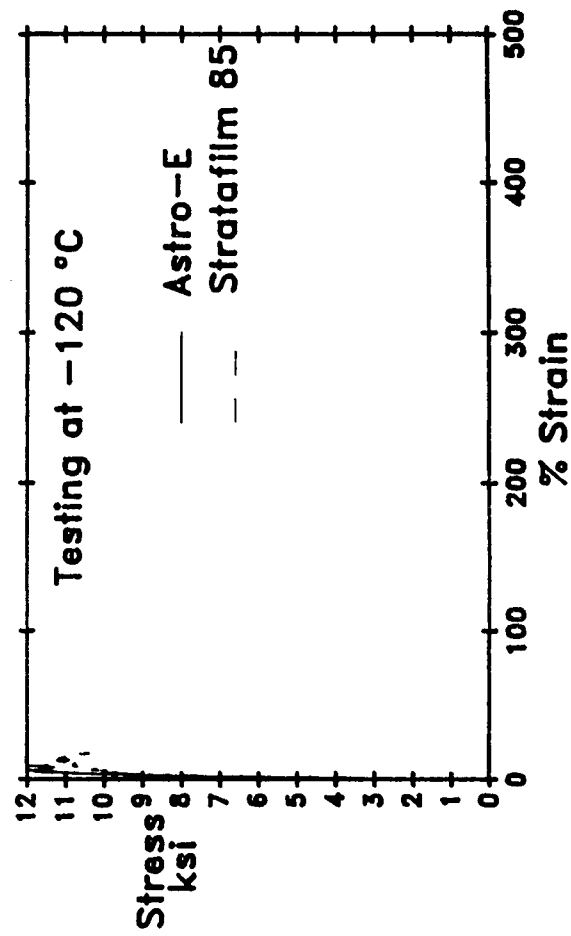
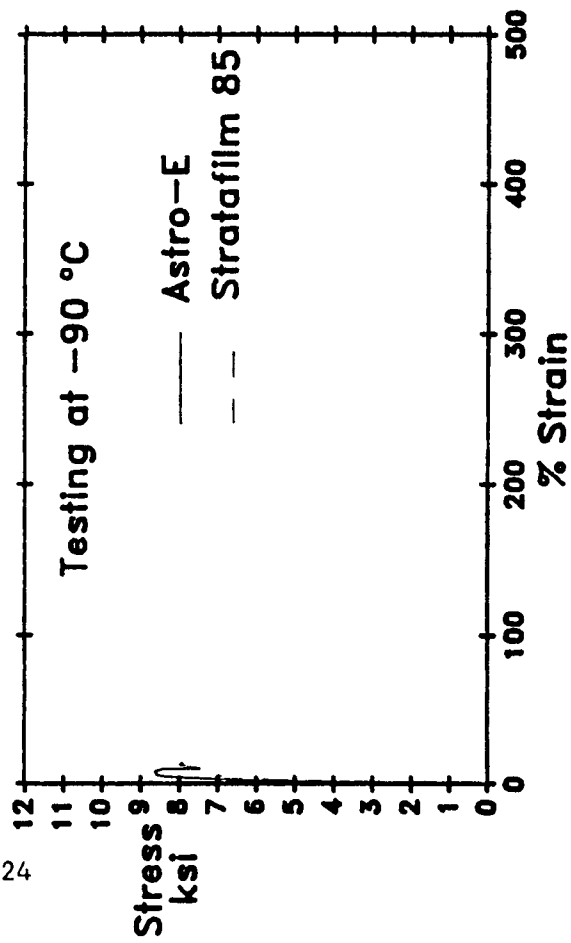
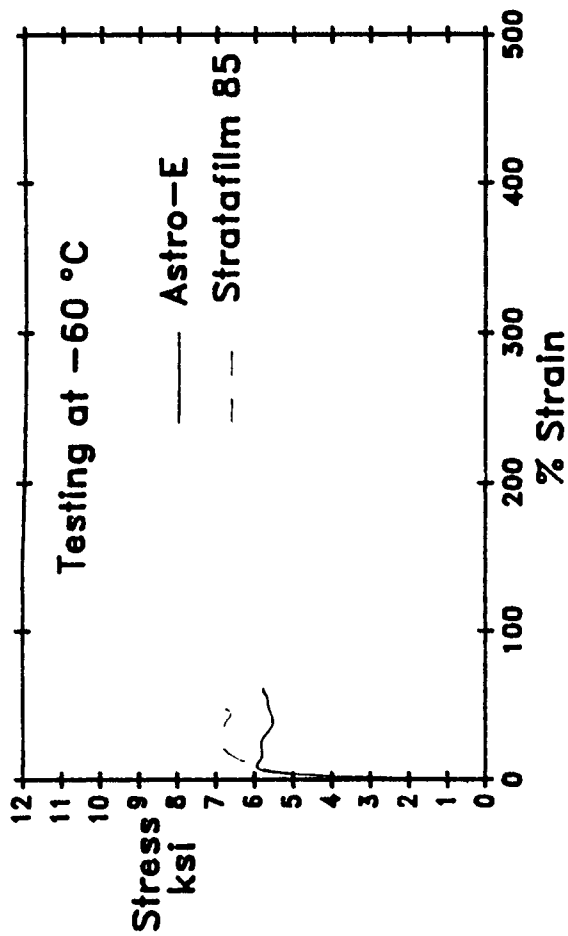
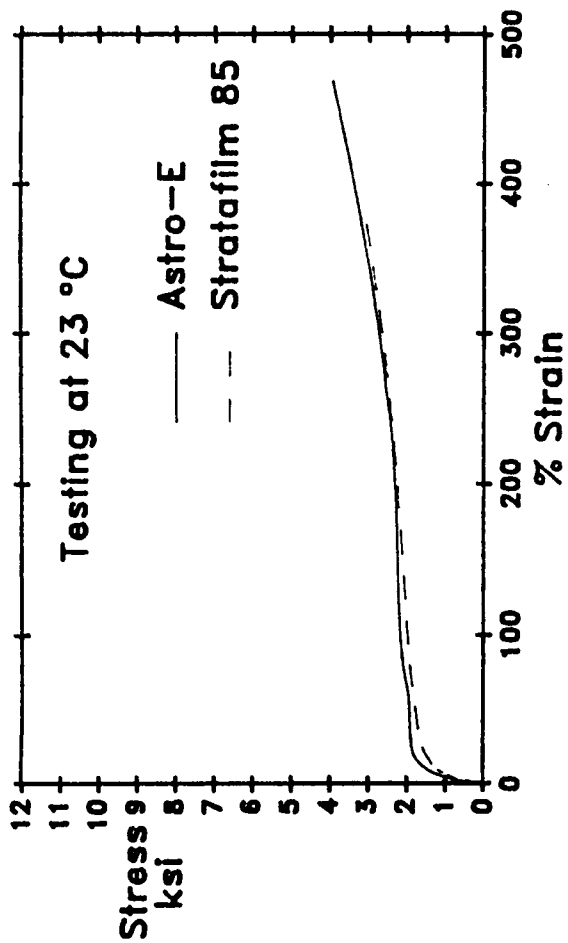


Fig 4: A comparison of stress verses strain  
at each of the testing temperatures

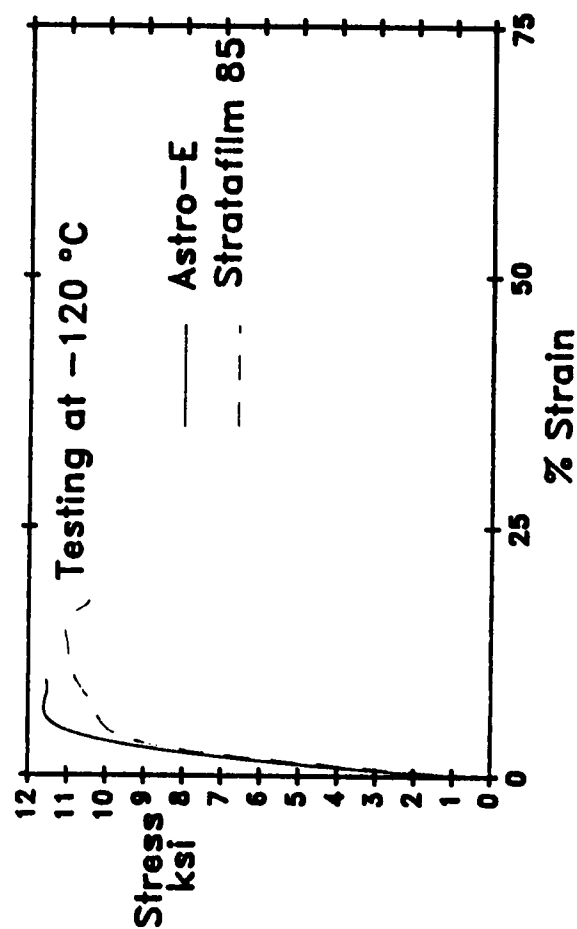
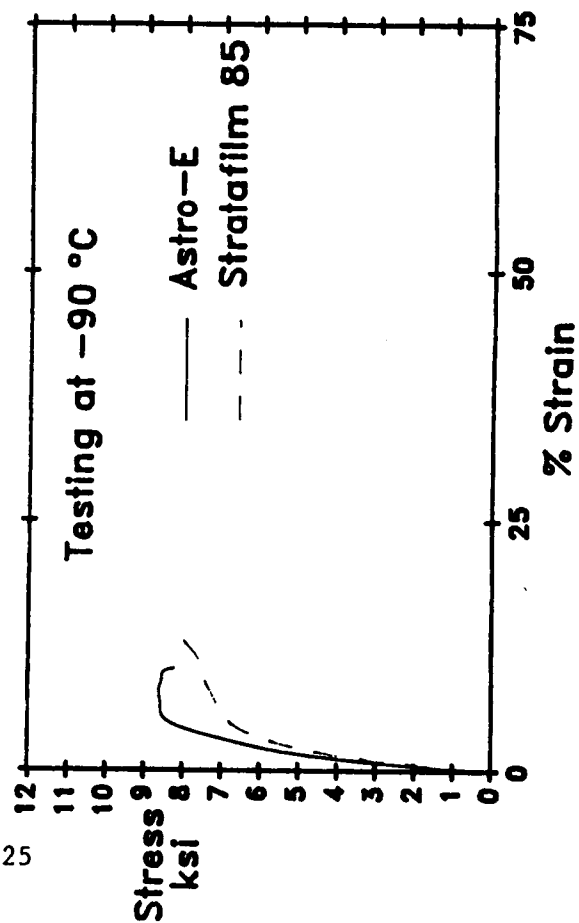
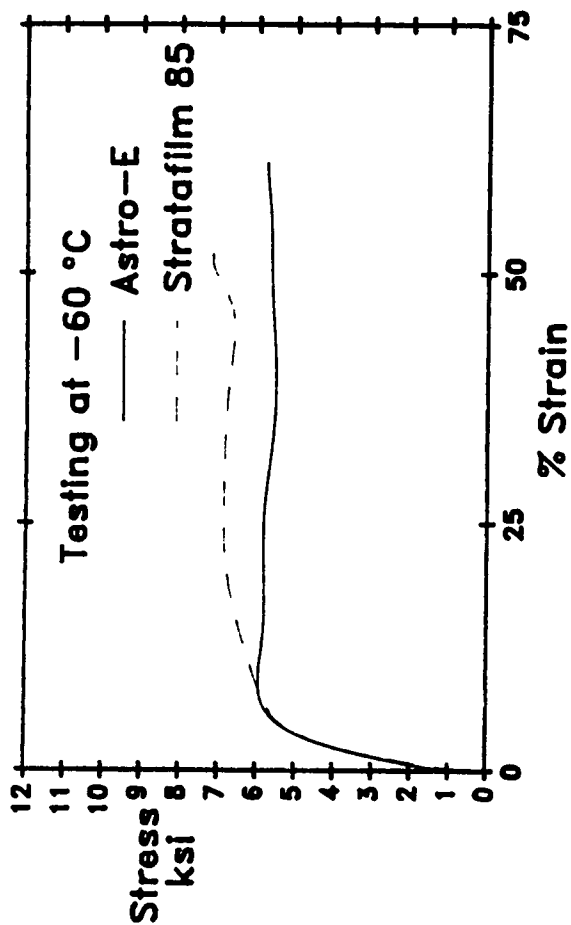
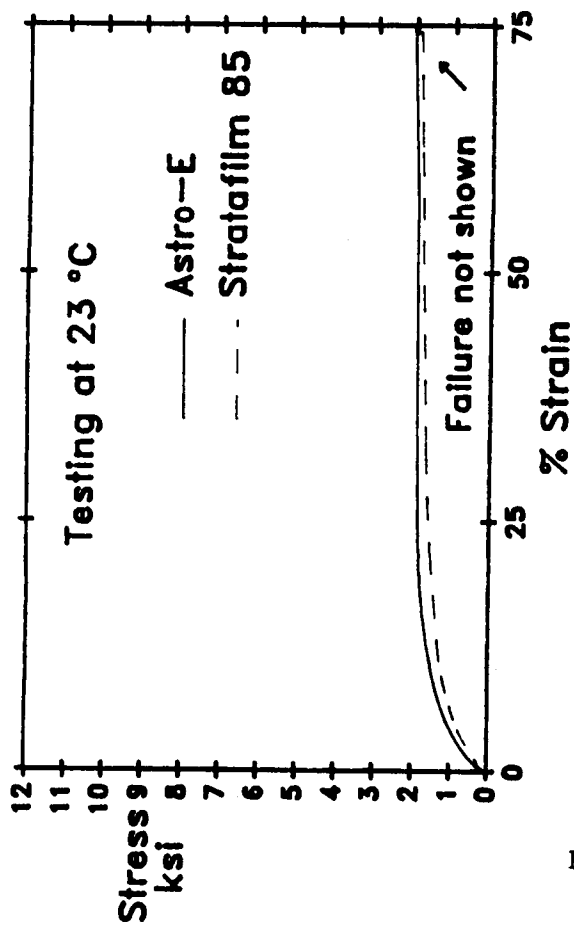


Fig 5: A comparison of stress verses strain  
on an expanded scale

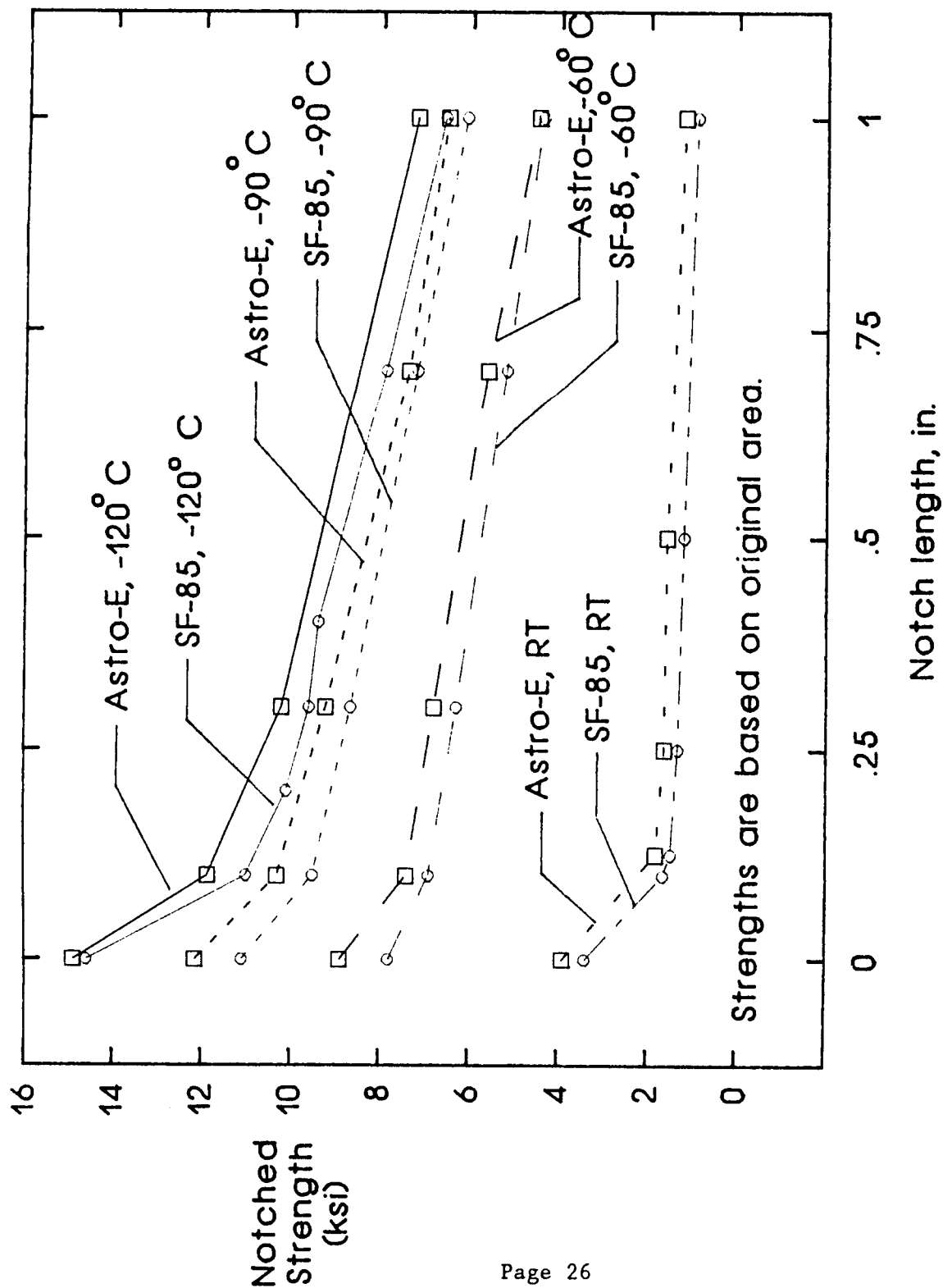


Fig 6: A plot of the Notched Strength verses Notch Length at each of the testing temperatures

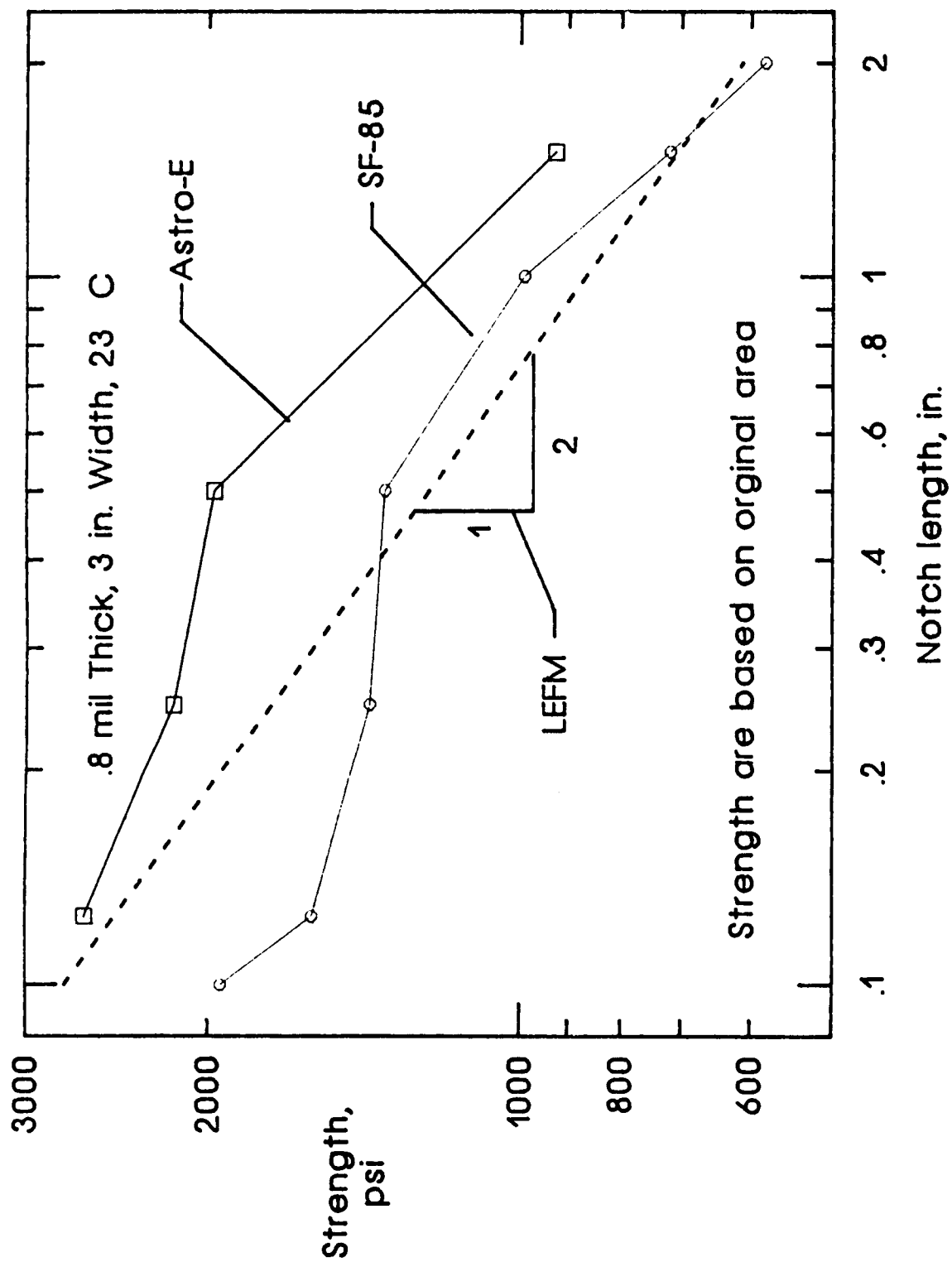


Fig 7: A comparison of Linear Elastic Fracture Mechanics to the plot of the failing strength verses notch length.

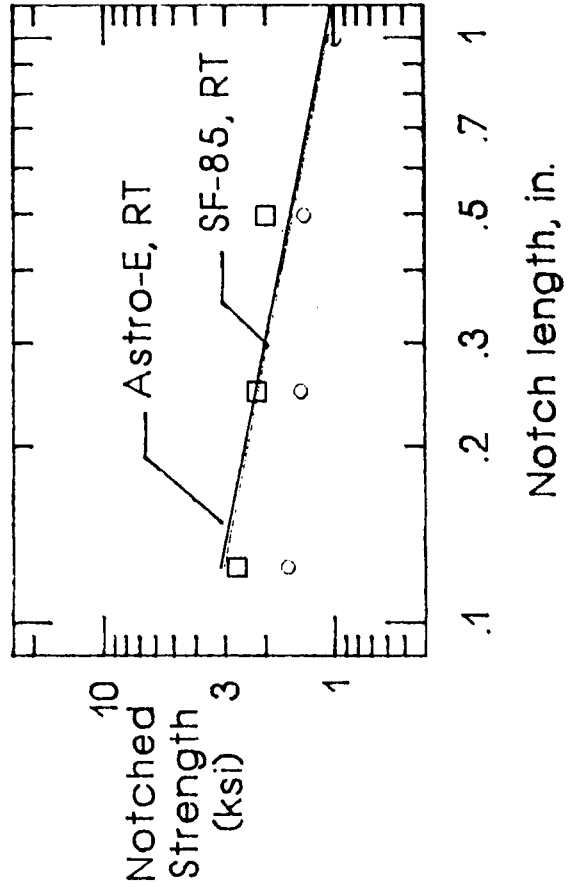
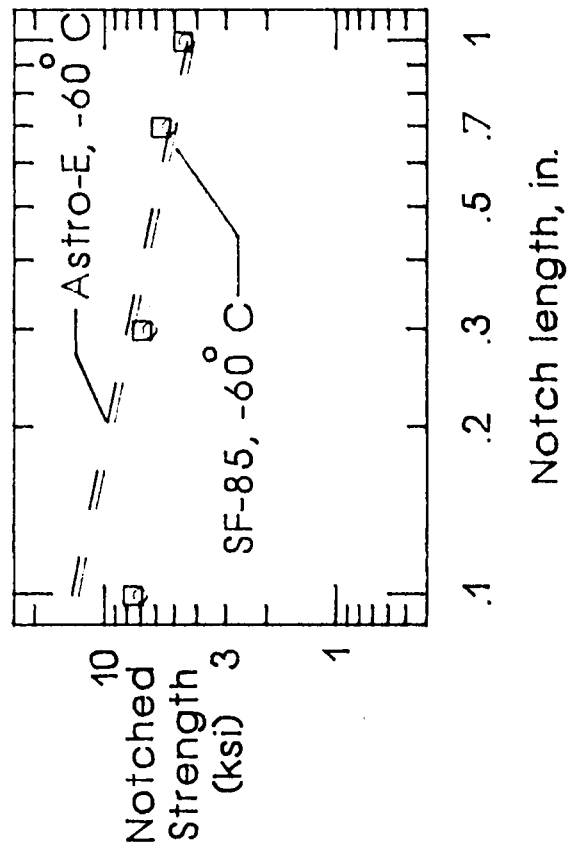
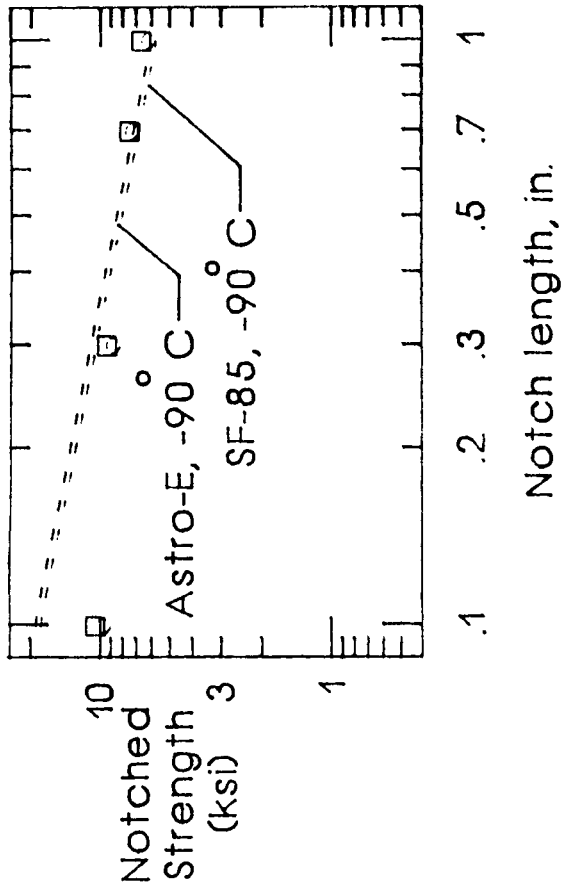
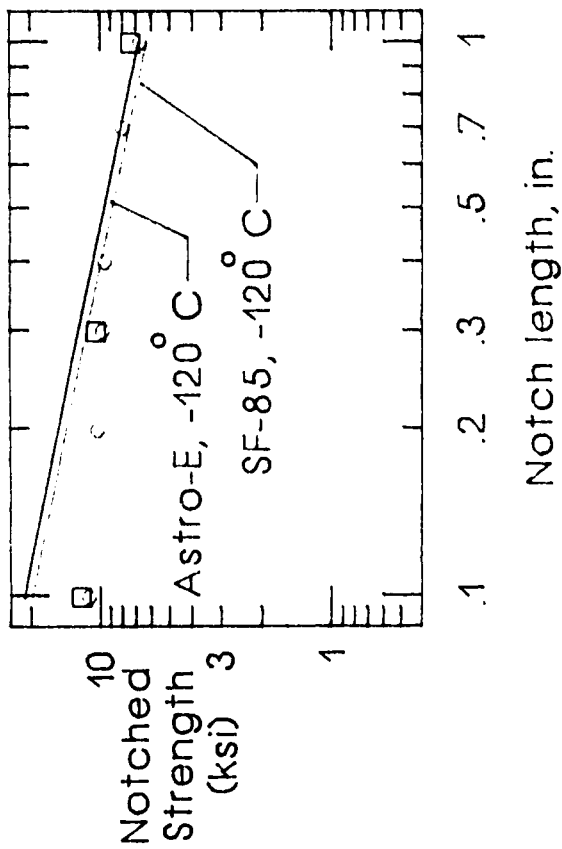


Fig 8: A plot of the notched strength verses notch length at each testing temperature

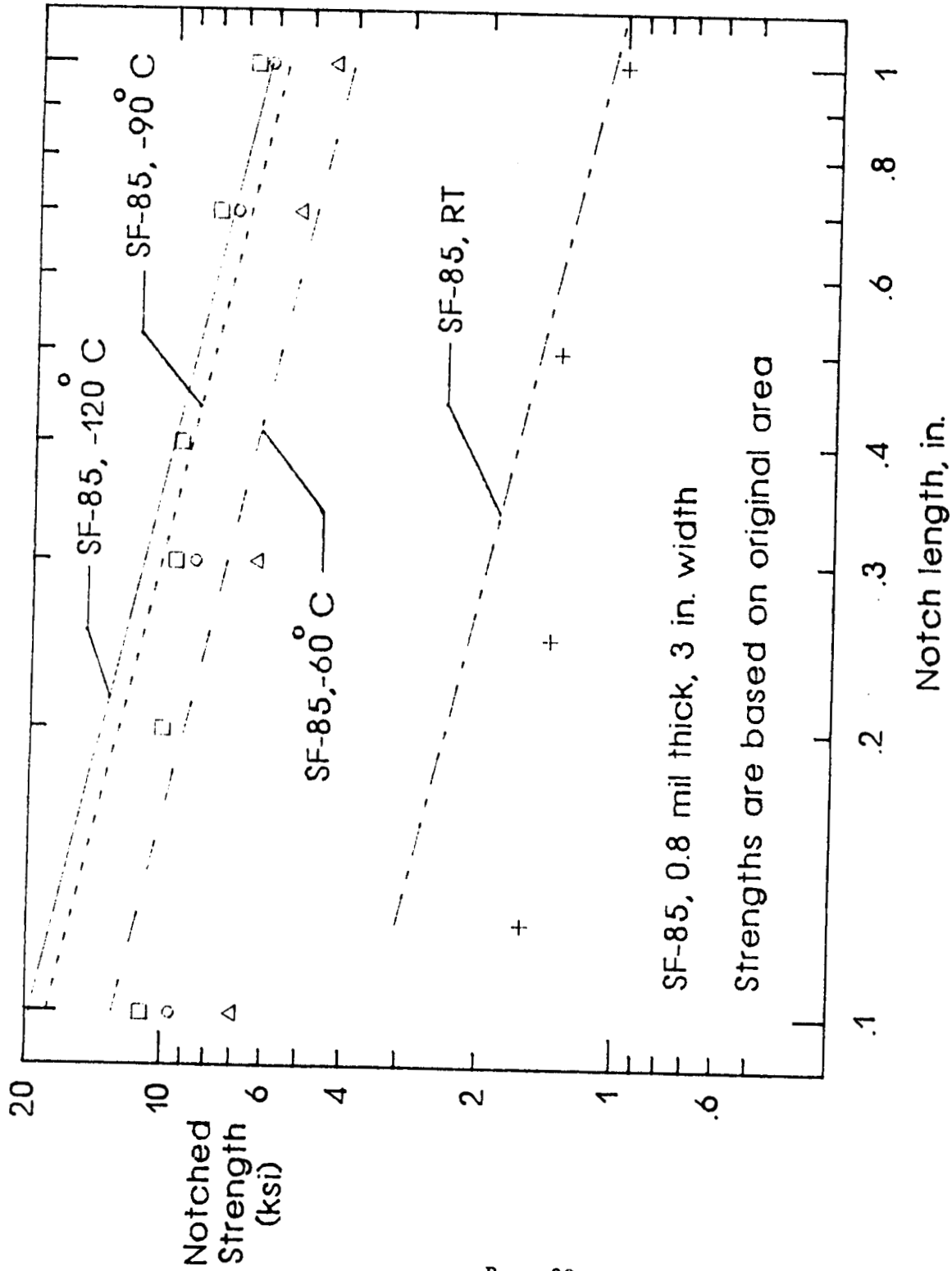


Fig 9: The notched strength of Stratafilm at each temperature  
with regression lines based on LEFM.

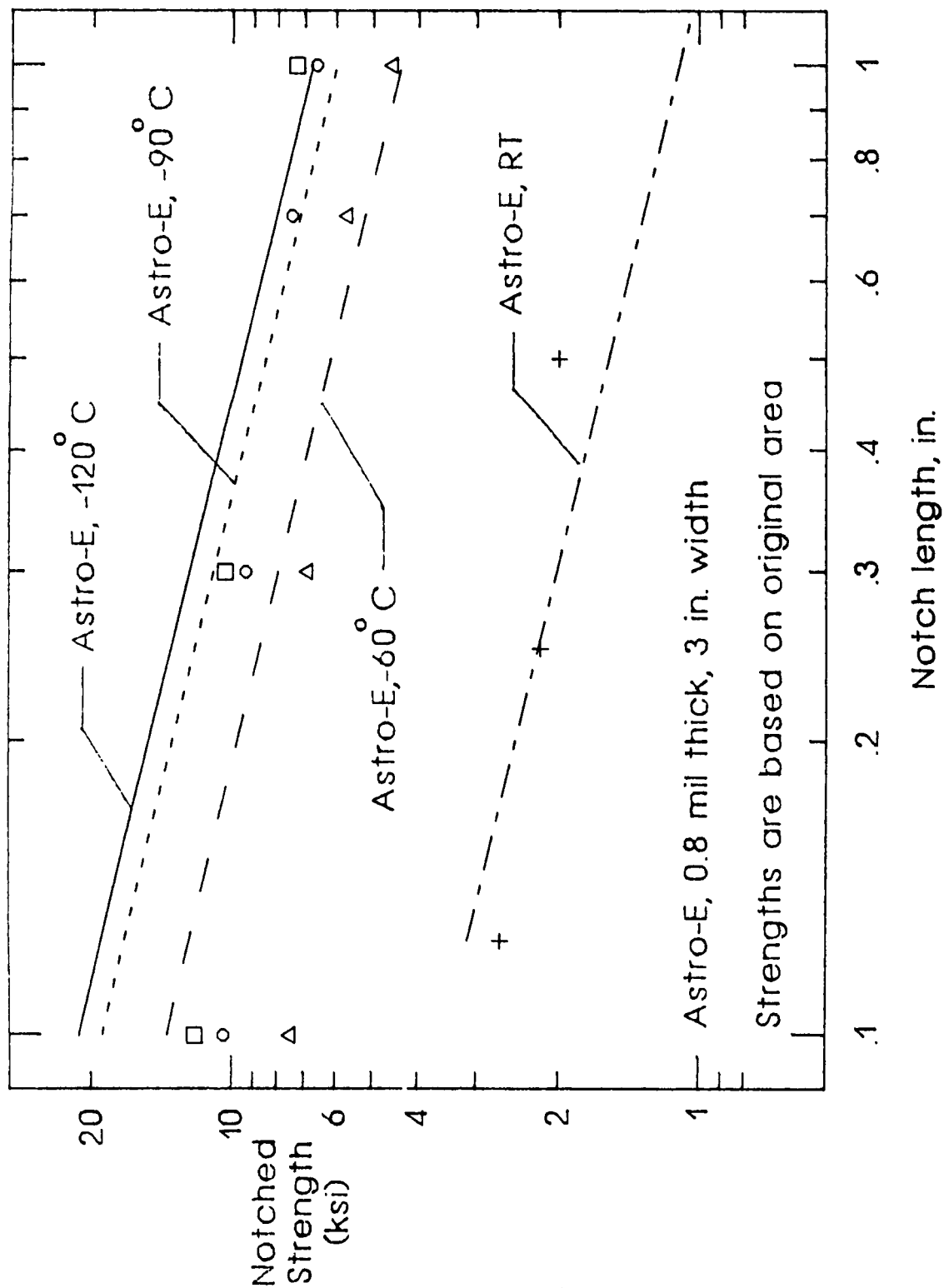


Fig 10: The notched strength of Astrofilm-E at each temperature.  
with regression lines based on LEFM.



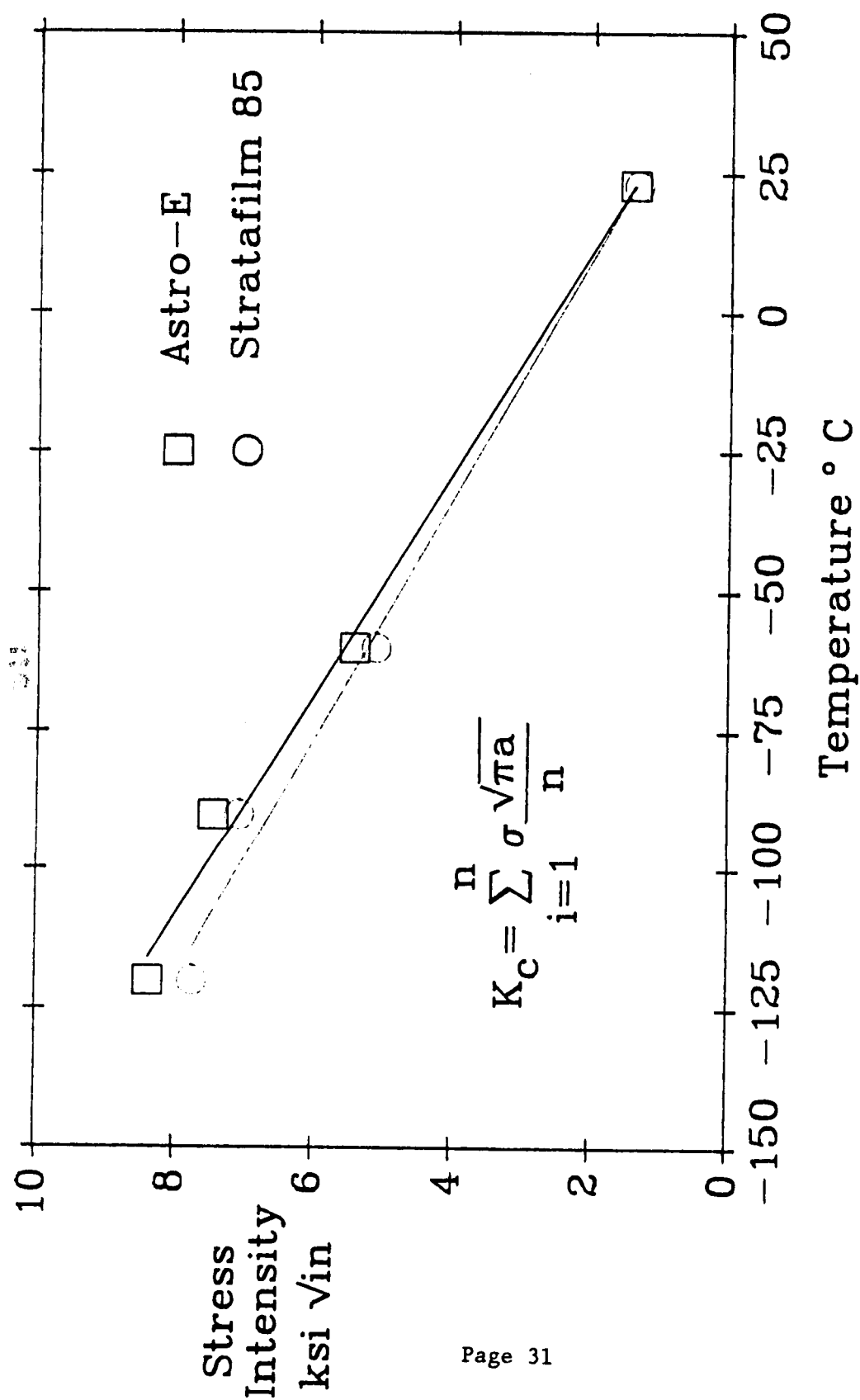
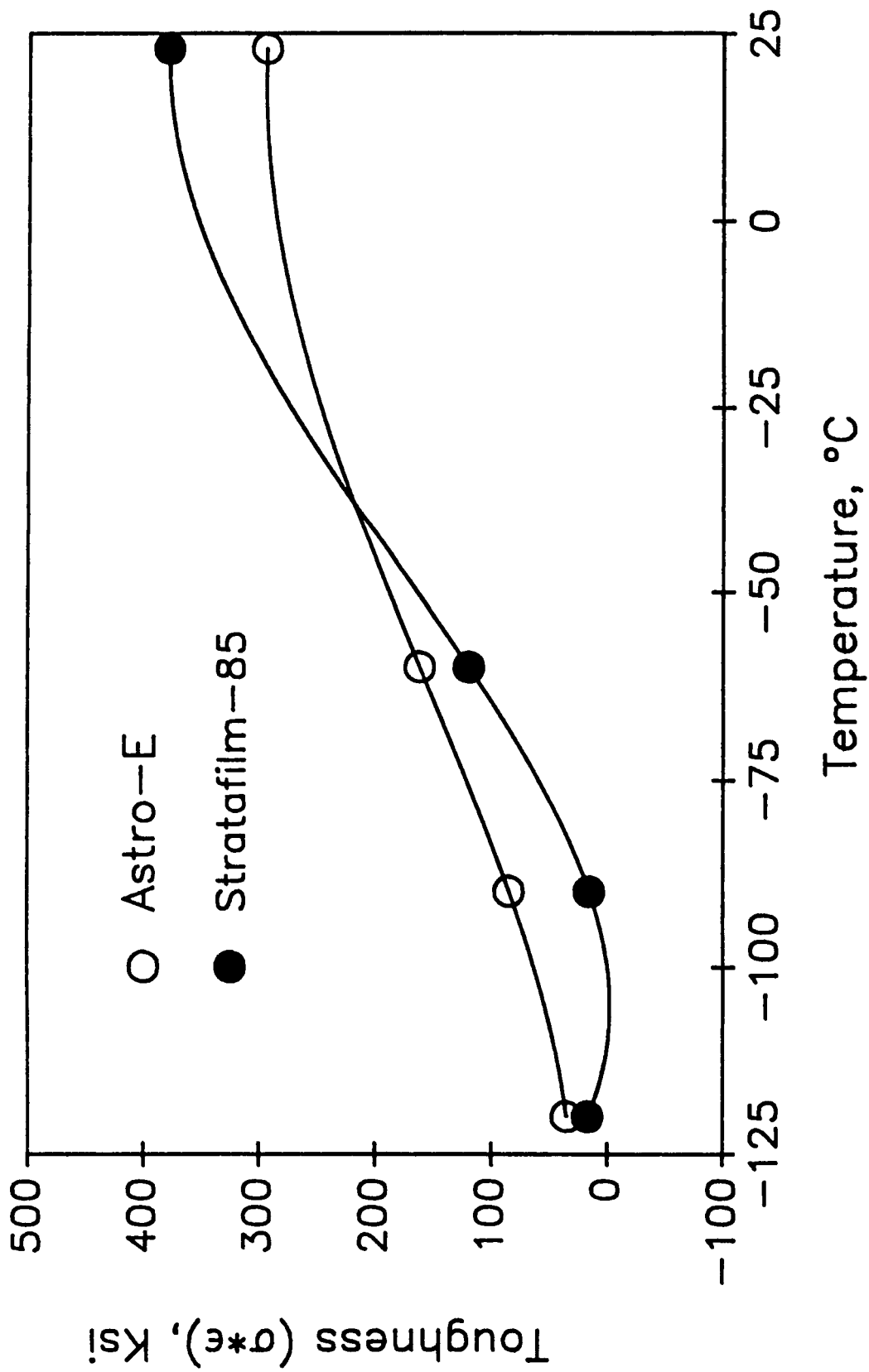


Fig 11: A plot of fracture toughness as a function of temperature



**Figure 12: A plot of the Modulus of Toughness  
verses Temperature**

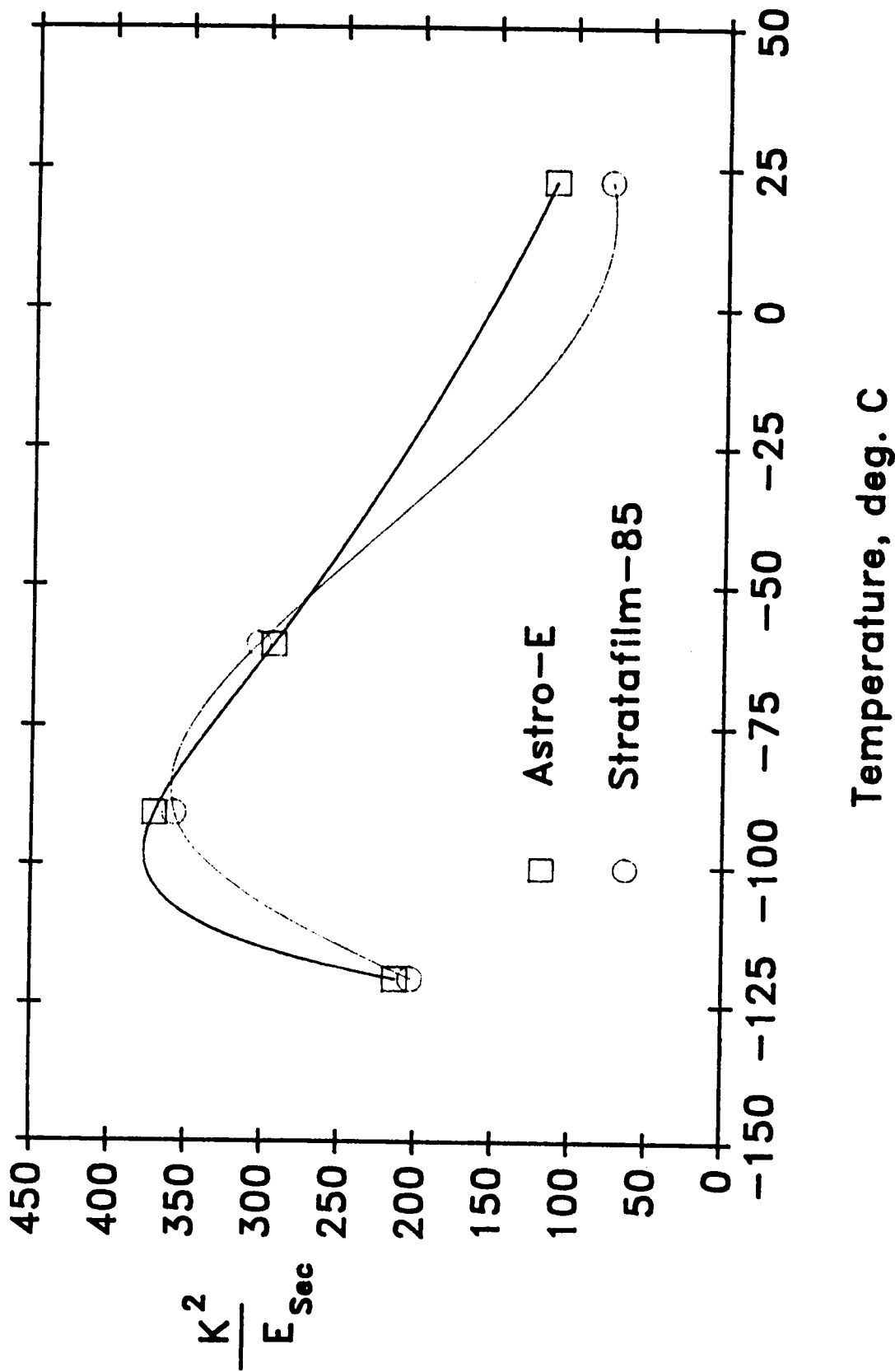


Figure 13: A plot of the pseudo strain energy release rate verses temperature.



## Report Documentation Page

1. Report No.  NASA CR-181686	2. Government Accession No.	3. Recipient's Catalog No.	
4. Title and Subtitle  Fracture Characteristics of Balloon Films		5. Report Date  January 1989	
		6. Performing Organization Code	
7. Author(s)  Marc A. Portanova		8. Performing Organization Report No.	
		10. Work Unit No.  505-63-01-05	
9. Performing Organization Name and Address  PRC Kentron, Inc. Hampton, VA 23666		11. Contract or Grant No.  NAS1-18000	
		13. Type of Report and Period Covered  Contractor Report	
12. Sponsoring Agency Name and Address  National Aeronautics and Space Administration Langley Research Center Hampton, VA 23665-5225		14. Sponsoring Agency Code	
15. Supplementary Notes  Langley Technical Monitor: C. C. Poe, Jr.			
16. Abstract  An attempt was made to determine the failure modes of high altitude scientific balloons through an investigation of the fracture characteristics of the thin polyethylene films. Two films were the subject of the evaluation, Winzen Int.'s Stratafilm SF-85 and Raven Industries' Astro-E.  Research began with an investigation of the film's cold brittleness point and it's effect on the ultimate strength and elasticity of the polyethylene film. A series of preliminary investigations were conducted to develop an understanding of the material characteristics. The primary focus of this investigation was on the notch sensitivity of the films. Simple stress strain tests were also conducted to enable analysis employing fracture toughness parameters. Studies were conducted on both film types at 23°C (room temperature), -60°C, -90°C, and -120°C.			
17. Key Words (Suggested by Author(s)) High altitude balloons Polyethylene film Notch sensitivity Crack propagation Tropopause		18. Distribution Statement  Unclassified - Unlimited Subject Category - 27	
19. Security Classif. (of this report)  Unclassified	20. Security Classif. (of this page)  Unclassified	21. No. of pages  35	22. Price  A03